UCLA
UCLA Previously Published Works

Title
Inverse estimates of anthropogenic CO2 uptake, transport, and storage by the ocean

Permalink
https://escholarship.org/uc/item/7n83j7gs

Journal
Global Biogeochemical Cycles, 20(2)

ISSN
0886-6236

Authors
Fletcher, SEM
Gruber, N
Jacobson, A R
et al.

Publication Date
2006-04-01

DOI
10.1029/2005GB002530

Peer reviewed

Inverse estimates of anthropogenic CO_2 uptake, transport, and storage by the ocean

S. E. Mikaloff Fletcher,[1,2] N. Gruber,[1] A. R. Jacobson,[3] S. C. Doney,[4] S. Dutkiewicz,[5] M. Gerber,[6] M. Follows,[5] F. Joos,[6] K. Lindsay,[7] D. Menemenlis,[8] A. Mouchet,[9] S. A. Müller,[6] and J. L. Sarmiento[3]

[1] Regional air-sea fluxes of anthropogenic CO_2 are estimated using a Green's function inversion method that combines data-based estimates of anthropogenic CO_2 in the ocean with information about ocean transport and mixing from a suite of Ocean General Circulation Models (OGCMs). In order to quantify the uncertainty associated with the estimated fluxes owing to modeled transport and errors in the data, we employ 10 OGCMs and three scenarios representing biases in the data-based anthropogenic CO_2 estimates. On the basis of the prescribed anthropogenic CO_2 storage, we find a global uptake of 2.2 ± 0.25 Pg C yr^{-1}, scaled to 1995. This error estimate represents the standard deviation of the models weighted by a CFC-based model skill score, which reduces the error range and emphasizes those models that have been shown to reproduce observed tracer concentrations most accurately. The greatest anthropogenic CO_2 uptake occurs in the Southern Ocean and in the tropics. The flux estimates imply vigorous northward transport in the Southern Hemisphere, northward cross-equatorial transport, and equatorward transport at high northern latitudes. Compared with forward simulations, we find substantially more uptake in the Southern Ocean, less uptake in the Pacific Ocean, and less global uptake. The large-scale spatial pattern of the estimated flux is generally insensitive to possible biases in the data and the models employed. However, the global uptake scales approximately linearly with changes in the global anthropogenic CO_2 inventory. Considerable uncertainties remain in some regions, particularly the Southern Ocean.

1. Introduction

[2] It is estimated that the Earth's oceans have absorbed about $48 \pm 9\%$ of the CO_2 emitted over the industrial period (1880–1994) from fossil fuel consumption and cement production [*Sabine et al.*, 2004]. Accurate, quantitative assessments of the spatial pattern of the air-sea flux of anthropogenic CO_2 are needed to improve our understanding of the physical processes controlling this uptake. However, there are substantial uncertainties associated with current estimates of these fluxes.

[3] The exchange of anthropogenic CO_2 across the air-sea interface cannot be measured directly. However, the total air-sea CO_2 exchange can be determined from observations of the difference between the partial pressures of CO_2 in the atmosphere and the surface ocean, pCO_2, and a formulation of the air-sea gas exchange coefficient [e.g., *Takahashi et al.*, 2002]. No method is currently available to measure the component of the air-sea exchange that is attributable to the anthropogenic perturbation of the atmospheric CO_2 concentration, although this quantity has been separated from the observations in the Indian Ocean using a method related to the one presented here [*Hall and Primeau*, 2004]. The spatial pattern of the oceanic uptake of anthropogenic CO_2 has traditionally been estimated using Ocean General Circulation Models (OGCMs) [e.g., *Orr et al.*, 2001; *Murnane et al.*, 1999; *Sarmiento et al.*, 1992].

[1]Department of Atmospheric and Oceanic Sciences and the Institute for Geophysics and Planetary Physics, University of California, Los Angeles, California, USA.

[2]Now at Atmospheric and Oceanic Sciences Program, Princeton University, Princeton, New Jersey, USA.

[3]Atmospheric and Oceanic Sciences Program, Princeton University, Princeton, New Jersey, USA.

[4]Marine Chemistry and Geochemistry, Woods Hole Oceanographic Institution, Woods Hole, Massachusetts, USA.

[5]Department of Earth, Atmosphere, and Planetary Sciences, Massachusetts Institute of Technology, Cambridge, Massachusetts, USA.

[6]Climate and Environmental Physics, Physics Institute, University of Bern, Bern, Switzerland.

[7]Climate and Global Dynamics Division, National Center for Atmospheric Research, Boulder, Colorado, USA.

[8]Estimating the Circulation and Climate of the Ocean (ECCO), Jet Propulsion Laboratory, Pasadena, California, USA.

[9]Astrophysics and Geophysics Institute, University of Liege, Liege, Belgium.

[4] The tracer-based ΔC^* method is used extensively to separate the concentration of anthropogenic CO_2 in the ocean from ocean interior observations of dissolved inorganic carbon (*DIC*) and other tracers [*Gruber et al.*, 1996]. This technique has been employed to calculate regional and global inventories of anthropogenic CO_2 storage in the ocean [e.g., *Lee et al.*, 2003; *Gruber*, 1998; *Sabine et al.*, 1999, 2002], and a global summary was presented by *Sabine et al.* [2004]. However, while this method provided many new insights into anthropogenic CO_2 storage, by itself it cannot be used to quantitatively assess the air-sea fluxes and oceanic transport of anthropogenic CO_2.

[5] Recently, an approach has been developed to estimate surface fluxes from ocean interior data [*Gloor et al.*, 2001; *Gruber et al.*, 2001; *Gloor et al.*, 2003]. This approach uses a Green's function inverse method analogous to atmospheric tracer inversions [e.g., *Enting and Mansbridge*, 1989; *Tans et al.*, 1990; *Bousquet et al.*, 2000] to infer regional air-sea fluxes from ocean interior observations and OGCMs that are used to determine how surface fluxes influence tracer concentrations in the interior ocean.

[6] The inverse approach is appealing because the flux estimates are driven by data and because it is independent of bulk formulations, such as the parameterization of the air-sea gas exchange coefficient needed to estimate air-sea fluxes from measurements of the air-sea partial pressure difference [e.g., *Takahashi et al.*, 2002]. The application of this inversion method to the anthropogenic CO_2 problem is aided by the fact that the large-scale spatial footprints of anthropogenic CO_2 uptake are well preserved in the oceans owing to the long timescales of ocean circulation. However, there are several important sources of uncertainty associated with this method that have not been addressed. Comparisons between heat and oxygen flux estimates using three different OGCMs suggested that model transport is one of the largest sources of uncertainty in the inverse estimates [*Gloor et al.*, 2001; *Gruber et al.*, 2001]. There are also several sources of uncertainty associated with the estimates of anthropogenic CO_2 used to constrain the inversion [*Gruber et al.*, 1996; *Matsumoto and Gruber*, 2005; *Keeling*, 2005; *Sabine and Gruber*, 2005]. A third issue that needs to be considered is the aggregation error, which is caused by the assumption that fluxes within a large spatial region are proportional to a prescribed spatial pattern [*Kaminski et al.*, 2001]. In addition, the inversion implicitly assumes that ocean circulation was approximately steady over the last 2 centuries and that the only source of temporal variability in the oceanic uptake of anthropogenic CO_2 is the atmospheric CO_2 perturbation.

[7] The aim of this paper is to extend the first estimates of *Gloor et al.* [2003] by estimating the air-sea fluxes of anthropogenic CO_2 with a refined method, address the uncertainties and robustness of these estimates, and explore the oceanic transport of anthropogenic CO_2 implied by the surface fluxes. We employ a suite of 10 OGCMs to estimate regional anthropogenic CO_2 fluxes from 24 regions. We discuss the features of the flux estimates and their implications for the global CO_2 cycle. We then explore the role of ocean transport in the inversion and assess the uncertainty due to differences among OGCMs. In addition, we quantify the effect of likely sources of systematic error in the data-based estimates of anthropogenic CO_2 on the inversely estimated fluxes. Finally, the inverse results are compared with forward model simulations using the same suite of models permitting us to assess what we have learned using the inverse approach.

2. Methods

2.1. Anthropogenic CO_2 Estimates

[8] One of the primary components enabling this work is the recent availability of a high-density, global data set of DIC and other tracers in the ocean interior from the Global Ocean Data Analysis Project (GLODAP) [*Key et al.*, 2004]. This data set is composed of data collected from cruises conducted as part of the World Ocean Circulation Experiment (WOCE), the Joint Global Ocean Flux Study (JGOFS), and the National Oceanic and Atmospheric Administration (NOAA) Ocean-Atmosphere Exchange Study (OACES) as well as historical cruises. (Locations of the observations are shown in Figure fs01 of the auxiliary material[1].) As a result of this project, over 68,000 observations are available to constrain the flux estimates.

[9] For each of these observations, the component of the observed DIC concentration that is due to the atmospheric perturbation of CO_2 was estimated using the ΔC^* method [*Gruber et al.*, 1996]. In this study, we use individual data points rather than the gridded data set. The spatial and temporal inhomogeneity of these data are accounted for by sampling the model simulated basis functions at the grid box corresponding to the sampling site during the year the data was collected, as discussed in the following section.

[10] A zonally averaged section of the reconstructed anthropogenic CO_2 used to constrain the inversion is shown in Figure 1. The highest anthropogenic CO_2 concentrations occur near the surface with generally rapidly decreasing concentrations toward the interior of the ocean. This is a consequence of the long timescale of ocean transport from the surface to the deep ocean interior. The deepest penetration occurs in the North Atlantic, owing to the extensive deep water formation in this region, and at midlatitudes, owing to the convergence of intermediate waters and mode waters that were recently in contact with the surface. There is little penetration in the tropics owing to the shallow thermocline. The anthropogenic CO_2 data set is discussed in detail by *Sabine et al.* [2004].

2.2. Inverse Model

[11] We use the same approach used by *Gloor et al.* [2003], with a few adaptations. We provide here only an overview of the method and refer to the auxiliary material for further details. The surface of the ocean is divided into 30 regions, and later aggregated to 24 regions as shown in Figure 2. Ten OGCMs are used to simulate a basis functions for each surface region, describing how an arbitrary unit of flux at the surface impacts tracer concentrations in the interior ocean. (Basis functions for one OGCM

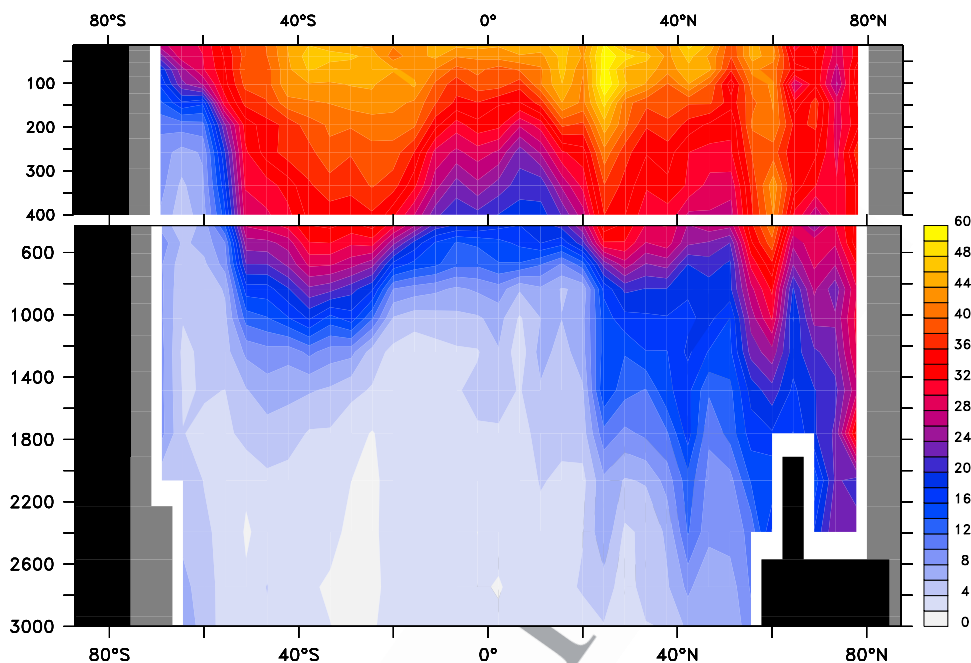[1]Auxiliary material is available at ftp://ftp.agu.org/apend/gb/2005GB002530.

Figure 1. Meridional section of zonally averaged anthropogenic CO_2 (μmol kg^{-1}) used to constrain the inversion. Uniform gray areas bounded by a thick, white line represent locations where no observations are available and black areas represent topography. Anthropogenic CO_2 was estimated from dissolved inorganic CO_2 measurements using the ΔC^* method of *Gruber et al.* [1996]. Based on data provided by GLODAP [*Key et al.*, 2004].

corresponding to each region are shown in Figure fs02 of the auxiliary material.) The resulting simulated basis functions are then sampled at the location and time of each of the observations during the year that each observation was collected (Figure 1). Each of the observations, in this case data-based estimates of anthropogenic CO_2, C_{ant}, is approximated as a linear combination of the *nreg* = 30 basis functions,

$$C_{ant} = \sum_{i=1, nreg} \lambda_i A_i + \varepsilon, \qquad (1)$$

where A_i is the modeled basis function concentration at the location of the observations, λ_i is a dimensionless factor that scales the unit surface flux into the region, and ε is a residual due to limitations of the method. In order to account for random errors in the data-based anthropogenic CO_2 estimates, each of the data-based estimates is weighted by the inverse of its random error, estimated by error propagation [see *Gruber et al.*, 1996]. Finally, the system of linear equations is solved for the combination of surface fluxes that is in optimal agreement with the data-based anthropogenic CO_2 estimates, using Singular Value decomposition (SVD). In cases where multiple observations occur in the same model grid box, each observation is treated as a separate constraint in the system of linear equations.

[12] The basis function for a given model region is generated by continuously injecting an arbitrary unit flux of a dye tracer into the surface of a this region and by running the OGCMs forward in time over the industrial period (1765−2005). This flux is distributed within the

region on the basis of the seasonal climatology of *Takahashi et al.* [2002] and scaled with time on the basis of the atmospheric CO_2 perturbation using a scaling factor, $\phi(t)$.

[13] The temporal scaling, ϕ, is calculated from the atmospheric CO_2 mixing ratio as done by *Gloor et al.* [2003].

$$\phi(t) = \frac{\chi_{CO_2}(t) - \chi_{CO_2}^{Preindustrial}}{\int \left(\chi_{CO_2}(t) - \chi_{CO_2}^{Preindustrial} \right) dt}, \qquad (2)$$

where χ_{CO_2} is the atmospheric mixing ratio of CO_2, assumed to be 280 ppm in preindustrial times [*Etheridge et al.*, 1996]. The time history of χ_{CO_2} is prescribed by a spline fit determined by *Enting et al.* [1994] on the basis of ice core data [*Neftel et al.*, 1985; *Friedli et al.*, 1986] and observations of atmospheric CO_2 at Mauna Loa Observatory [*Keeling et al.*, 1989]. We updated this time series to the year 2005 using observations from Mauna Loa provided by CMDL/NOAA and a scaled version of the IS92 scenario [*Mikaloff Fletcher et al.*, 2003]. Here $\chi_{CO_2}^{Preindustrial}$ is 280 ppm based on ice core data.

[14] This temporal scaling of the dye fluxes is possible owing to the nearly exponential growth of atmospheric CO_2 during the industrial period. Theoretical considerations and a box model analysis show that when the mixing ratio of an atmospheric gas increases exponentially, the oceanic uptake is, to first order, proportional to the rate of growth. This is because the atmospheric growth rate of a trace gas at any point in time is proportional to the total amount of the trace gas in the atmosphere. We confirmed our scaling by plotting
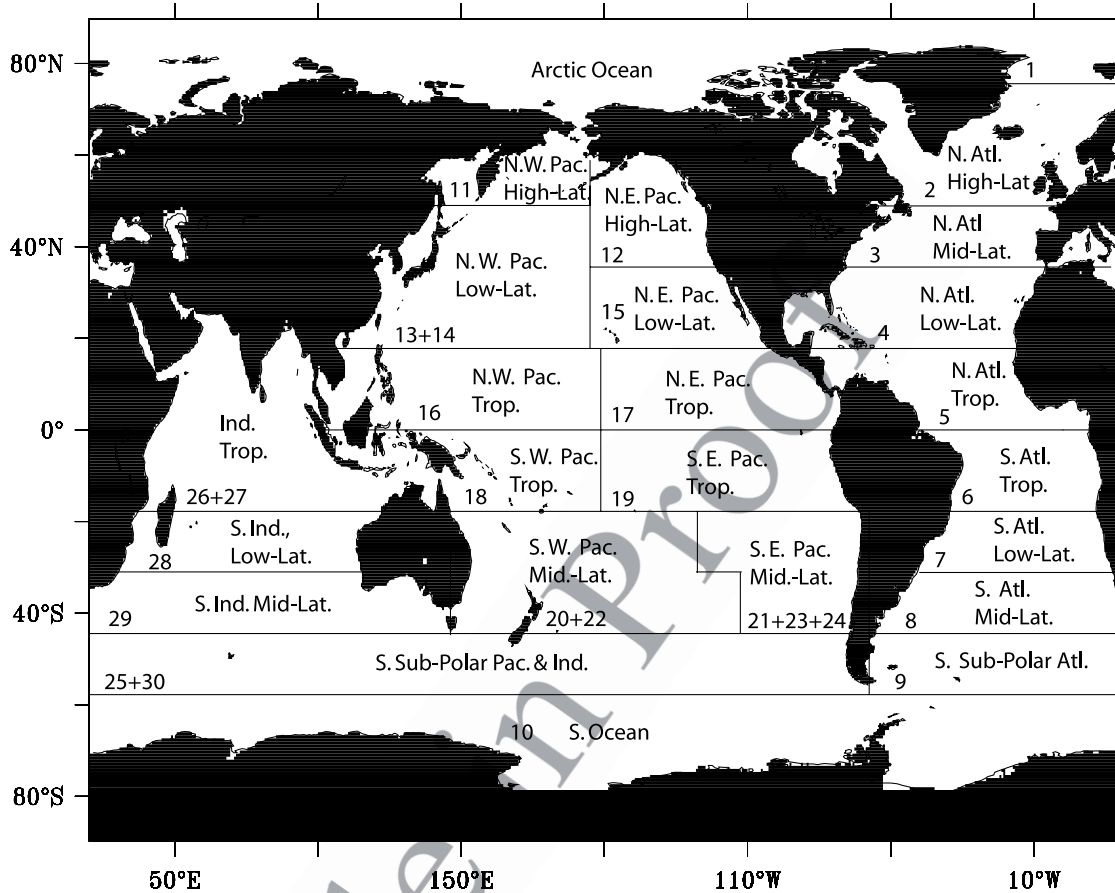
Figure 2. The 24 regions used for the ocean inversion. The region numbers show the aggregation from the original 30 regions [*Mikaloff Fletcher et al.*, 2003] to the 24 regions used in this study.

231 anthropogenic CO$_2$ uptake versus atmospheric CO$_2$ pertur-
232 bation using results from the second phase of the Ocean
233 Carbon-cycle Model Intercomparison Project (OCMIP-2)
234 [*Watson and Orr*, 2003] (see Figure fs03 of the auxiliary
235 material). This analysis also reveals some notable departures
236 from our scaling around 1800 and 1940. These are caused
237 by the large changes in atmospheric CO$_2$ growth rate that
238 occurred during these periods. The results from the
239 OCMIP-2 forward simulations also demonstrate that the
240 increase in the buffer factor due to the accumulation of
241 anthropogenic CO$_2$ in the surface ocean between 1765 and
242 2005 is too small to have caused a detectable deviation from
243 our assumed linear scaling.

244 [15] Basis functions were computed for 30 surface regions
245 [*Mikaloff Fletcher et al.*, 2003], and later aggregated to
246 24 regions. These aggregations were selected to minimize
247 the covariance between the modeled response to surface
248 fluxes into each pair of regions. High covariances between
249 regions indicate that the inversion cannot effectively distin-
250 guish between two regions either because the basis func-
251 tions are too similar or because the observational data set is
252 insufficient. The sum of the fluxes into two regions with
253 high covariance may be well constrained, but the individual
254 fluxes are highly uncertain.

2.3. OGCMs

[16] We employ basis functions from 10 OGCMs in order
to elucidate the role of differences in OGCM transport in the
inversion. These model simulations were undertaken by six
different modeling groups: Princeton (PRINCE) Massachu-
setts Institute of Technology (MIT), Bern-Switzerland
(Bern3D), Jet Propulsion Laboratory (ECCO), National
Center for Atmospheric Research (NCAR), and University
of Liége-Belgium (UL) (described briefly in the auxiliary
material). Princeton provided results from five different
configurations of their model [*Gnanadesikan et al.*, 2002,
2004], summarized in Table ts01 of the auxiliary material.
Owing to the history of model development, several of these
models share common numerical cores. However, compar-
ison with data constraints have shown that differences in
sub-grid-scale parameterizations and surface forcing are a
stronger determinant of model differences than model
architecture [*Dutay et al.*, 2002; *Doney et al.*, 2004;
Matsumoto et al., 2004]. This is well illustrated by the
PRINCE family of models, which share the same funda-
mental numerical core setup, but have differing values of
the vertical and along-isopycnal diffusivity, and in some
cases also differing salinity restoring schemes, wind fields,
and topography. These changes cause the resulting model

t1.1 **Table 1.** Evaluation of Model Skill Based on Comparisons Between CFC-11 Model Simulations and the GLODAP Gridded CFC Data Set[a]

t1.2		Correlation	Normalized Std. Dev.[b]	Model Skill[c]	Inverse Anthropogenic CO_2 Uptake, Pg C yr^{-1}	Forward Anthropogenic CO_2 Uptake, Pg C yr^{-1}
t1.3	BERN	0.89	1.04	0.81	2.05	N.A.
t1.4	ECCO	0.96	0.89	0.91	2.01	N.A.
t1.5	MIT	0.91	1.00	0.85	2.22	N.A.
t1.6	NCAR	0.95	0.98	0.91	2.18	2.36
t1.7	PRINCE-LL	0.90	1.18	0.80	1.85	1.90
t1.8	PRINCE-HH	0.93	1.05	0.87	2.33	2.43
t1.9	PRINCE-LHS	0.93	1.04	0.86	1.99	2.04
t1.10	PRINCE-2	0.93	1.03	0.87	2.17	2.24
t1.11	PRINCE-2a	0.91	1.05	0.85	2.25	2.35
t1.12	UL	0.87	1.0	0.77	2.81	2.95
t1.13	Mean	0.92	1.02	0.85	2.18	2.32

[a]Also tabulated are forward and inverse estimates of the global total anthropogenic CO_2 uptake (Pg C yr^{-1}, scaled to 1995).
t1.14 Forward results are from OCMIP-2 [*Dutay et al.*, 2002; *Watson and Orr*, 2003].
[b]Std. Dev. is defined as the standard deviation of the modeled field divided by the corresponding standard deviation of the
t1.15 observed field.
t1.16 [c]*Taylor* [2001].

configurations to span nearly the entire range of model behavior seen in the global coarse-resolution models that participated in OCMIP-2 [*Matsumoto et al.*, 2004].

[17] Four of the models used here have been compared in OCMIP-2 [*Dutay et al.*, 2002; *Doney et al.*, 2004; *Watson and Orr*, 2003]: the LL configuration of PRINCE, and the MIT, NCAR, and UL models. The MIT model used here has a slightly different configuration from the version used in OCMIP-2.

[18] In order to determine which models are likely to have the most accurate transport on the timescale of anthropogenic CO_2 perturbation, we compare the GLODAP gridded CFC-11 data set with simulations of CFC-11 from that followed the OCMIP-2 protocol [*Dutay et al.*, 2002]. Table 1 shows the correlation between the gridded CFC-11 data and the modeled CFC-11, the standard deviation of the modeled CFC-11 normalized by the standard deviation of the gridded CFC-11 data, and a CFC-11 model skill score based on these two quantities [*Taylor*, 2001]. We use these CFC-11 skill scores to weight the different models when calculating the between-model means and standard deviations, such that models that simulate the distribution of CFC-11 more accurately have a stronger effect on the reported results.

3. Results

3.1. Anthropogenic CO_2 Uptake

[19] The inversion finds a global anthropogenic CO_2 uptake of 2.2 Pg C yr^{-1}, with a weighted standard deviation of 0.25 Pg C yr^{-1}, scaled to a nominal year of 1995. The range across all models is 1.85 to 2.81 Pg C yr^{-1} (Table 1). This substantial range is due in part to differences between the effective vertical diffusivities in the models. Highly diffusive models distribute the dye over a larger portion of the ocean. This requires larger anthropogenic CO_2 fluxes in order to match the high observed anthropogenic CO_2 concentrations in the upper ocean. The OGCMs providing the high and low ends of this range (UL and PRINCE-LL) also have lower CFC-11 skill scores than the other OGCMs

used in this study. This suggests that the cross-model range can be considered an upper estimate of the uncertainty associated with the inversely estimated global anthropogenic CO_2 uptake.

[20] The greatest anthropogenic CO_2 uptake occurs in the Southern Ocean, particularly in the subpolar regions (44°S to 58°S), where the weighted mean anthropogenic CO_2 uptake is 0.51 Pg C yr^{-1} with a standard deviation of 0.17 Pg C yr^{-1} (Figure 3). This flux represents 23% of the global total anthropogenic CO_2 uptake. In addition, the inversion finds considerable anthropogenic CO_2 uptake in the tropics. In contrast, anthropogenic CO_2 uptake at mid latitudes is found to be low, despite the fact that the greatest anthropogenic CO_2 storage occurs there (Figure 1).

[21] These broad features in the spatial pattern of the fluxes are consistent across all of the models that participated in this study. However, there exists considerable model differences between the anthropogenic flux estimates for some regions, leading to substantial uncertainties in the weighted means. The greatest anthropogenic CO_2 uncertainty occurs in the Southern Ocean, with a weighted standard deviation from the weighted mean uptake of 0.10 Pg C yr^{-1} for the region south of 58°S and 0.17 Pg C yr^{-1} for the region between 44°S and 58°S. As a percentage of the total signal, the range in the high-latitude North Atlantic is also very high. The inverse estimates are the most consistent in the North Atlantic and North Pacific.

[22] This uptake pattern is in good agreement with previous forward modeling studies. In some of the first 3-D OGCM studies of the oceanic uptake of anthropogenic CO_2, *Sarmiento et al.* [1992] and *Maier-Reimer and Hasselmann* [1987] found a similar pattern of vigorous anthropogenic CO_2 uptake at high latitudes and at the equator, and low anthropogenic CO_2 uptake at midlatitudes. They attributed the high uptake in the tropics and in the high latitudes primarily to these regions being characterized by high rates of transport and mixing of subsurface waters depleted in anthropogenic CO_2 to the surface. Although variations in gas transfer velocity were found by *Sarmiento et al.* [1992] to be of second importance for the global uptake of
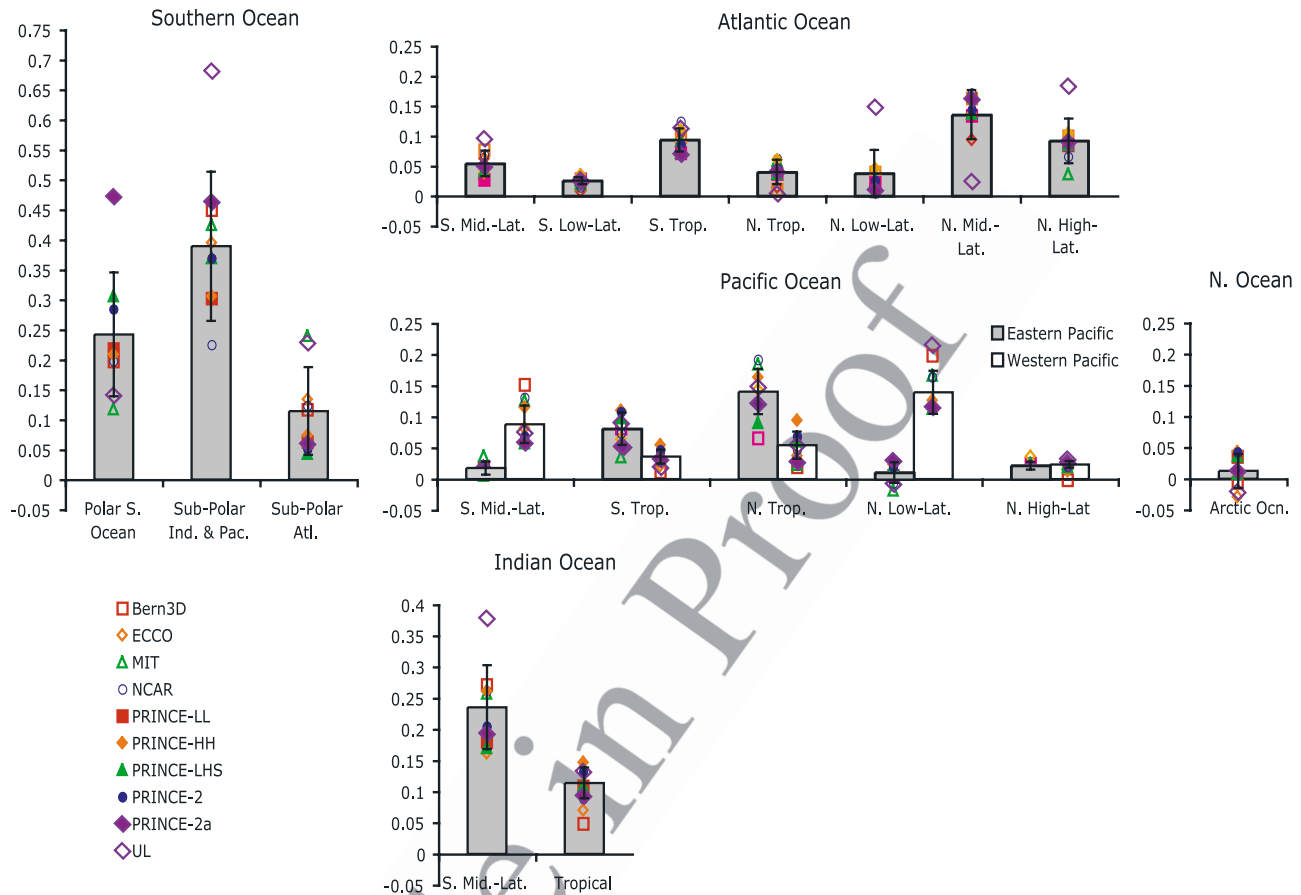
Figure 3. Inverse estimates of anthropogenic CO_2 uptake by the ocean (Pg C yr^{-1}) for a nominal year of 1995 (positive values indicate flux into the ocean). The columns show the cross-model weighted means, and the error bars represent the weighted standard deviation. The weights were provided by the model's CFC-11 skill scores (see Table 1). The flux estimates for individual models are shown as symbols.

anthropogenic CO_2, the higher wind speeds in high-latitude regions were found to have some enhancing effect on greater anthropogenic CO_2 uptake there. Owing to the long residence of upper ocean waters in the midlatitudes, anthropogenic CO_2 in the surface waters of these regions generally follows the atmospheric perturbation quite closely [see, e.g., *Gruber et al.*, 2002; *Keeling et al.*, 2004; *Takahashi*, 2004]. This leads to low uptake.

[23] *Sarmiento et al.* [1992] found an anthropogenic CO_2 uptake of 1.9 Pg C yr^{-1} for the decade from 1980 to 1989. This is comparable with our weighted estimate of 1.82 ± 0.21 Pg C yr^{-1} when scaled to the same time period. *Orr et al.* [2001] simulated anthropogenic CO_2 uptake using four 3-D OGCMs and found a 1980–1989 uptake of 1.85 ± 0.35 Pg C yr^{-1}. Like this study, they found the greatest anthropogenic CO_2 uptake and the greatest range between models in the Southern Ocean. The inverse estimates will be compared in more detail with the forward simulations in section 5.

[24] This study is also in good agreement with the earlier inversion study of *Gloor et al.* [2003] (Figure fs05 of the auxiliary material), as the latter estimates generally fall within the model range of this study. Since the methodology is the same, the primary causes for the differences between the two studies are the choice of OGCM and the selection of model regions. *Gloor et al.* [2003] used only one model (PRINCE-LL, also used here), while we report the weighted mean of 10 models, including the PRINCE-LL model. We estimate fluxes into 24 surface regions while *Gloor et al.* [2003] used only 13 regions. The larger number of model regions in this study is expected to reduce the aggregation error [*Kaminski et al.*, 2001], giving our results more confidence. In addition, we employ a spatial and temporal flux pattern modeled after the observationally based air-sea CO_2 flux estimates of *Takahashi et al.* [2002], which is likely a better assumption than the annual mean pattern based on heat fluxes employed by *Gloor et al.* [2003]. Additional but likely smaller differences between the two studies arise because we weight the data-based anthropogenic CO_2 estimates with an estimate of the random error, which is different for every observation, while *Gloor et al.* [2003] weighted all of the observations equally. Finally, a
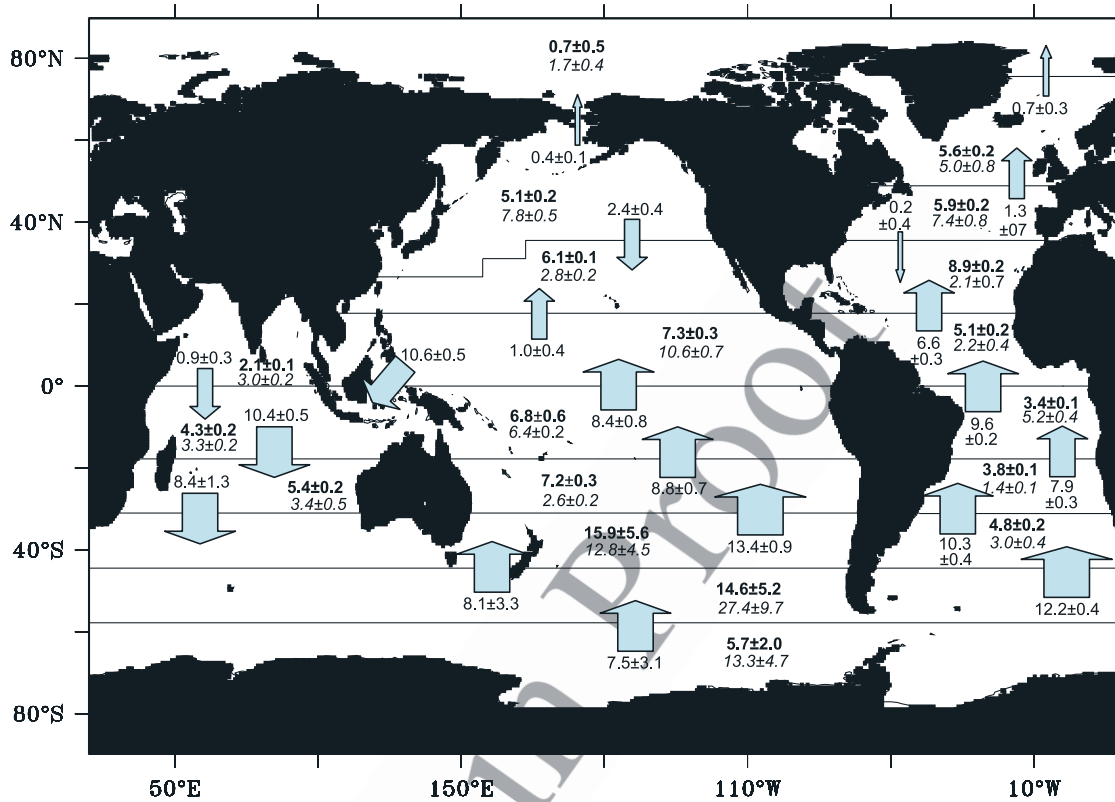
Figure 4. Global map of the time integrated (1765–1995) transport (shown above or below arrows) of anthropogenic CO_2 based on the inverse flux estimates (italics) and their implied storage (bold) in Pg C. Shown are the weighted mean estimates and their weighted standard deviation.

larger anthropogenic CO_2 data set is available to constrain the inverse estimates in this study. Owing to the large number of observations used in both studies, this latter difference has little impact on the inverse estimates.

3.2. Oceanic Transport of Anthropogenic CO_2

[25] The transport of anthropogenic CO_2 can be calculated from the divergence of the regional fluxes integrated in time (1765–1995) and the inverse storage estimates. In order to be consistent with the estimated fluxes, we calculated this storage from the sum of the regional scaling factors multiplied by the basis functions (equation (1)), rather than using observed storage.

[26] Globally, the vigorous anthropogenic CO_2 uptake in the Southern Ocean and the absence of large storage there drive a substantial equatorward transport in most of the Southern Hemisphere (Figure 4). Only about half of the anthropogenic CO_2 taken up in the high-latitude Southern Ocean is stored there, while the rest is transported equatorward. This leads to a considerable anthropogenic CO_2 storage at midlatitudes in the Southern Hemisphere and a northward cross-equatorial transport. In the Northern Hemisphere, anthropogenic CO_2 is transported poleward from the tropics and equatorward from midlatitudes, leading to convergence and storage in the subtropics. We find a small amount of poleward transport from high latitudes into the Arctic Ocean. This general pattern of anthropogenic uptake at high latitudes and in the tropics with subsequent transport

to midlatitudes, where the anthropogenic CO_2 is stored, is in good agreement with previous modeling studies [*Sarmiento et al.*, 1992].

[27] The largest portion of the anthropogenic CO_2 transported equatorward from the Southern Ocean is going into the Atlantic Ocean. Some of it is transported northward along the surface, and some of it is transported at depth, mostly associated with the equatorward and downward spreading of Sub-Antarctic Mode Water (SAMW) and Antarctic Intermediate Water (AAIW). The bulk of this Southern Ocean derived anthropogenic CO_2 then accumulates in the South Atlantic Subtropical Gyre (basis functions shown in Figures fs06 and fs07 of the auxiliary material). A portion of the anthropogenic CO_2 taken up in the tropics is transported southward, but most is either stored there or transported northward along the surface and then stored in the subtropical North Atlantic (Figure fs02 of the auxiliary material, regions 5 and 6).

[28] In the North Atlantic, the greatest anthropogenic CO_2 uptake occurs at mid and high latitudes. Anthropogenic CO_2 taken up in these regions is either transported equatorward to midlatitudes or poleward, where it is entrained into North Atlantic Deep Water (NADW) (Figure fs02 of the auxiliary material, regions 2 and 3). This leads to convergence and storage in the Northern Subtropics (Figure 4).

[29] About 40% of the anthropogenic CO_2 transported poleward from the Southern Ocean is going into the Pacific Ocean or into the Indian Oceans (Figure fs02 of the
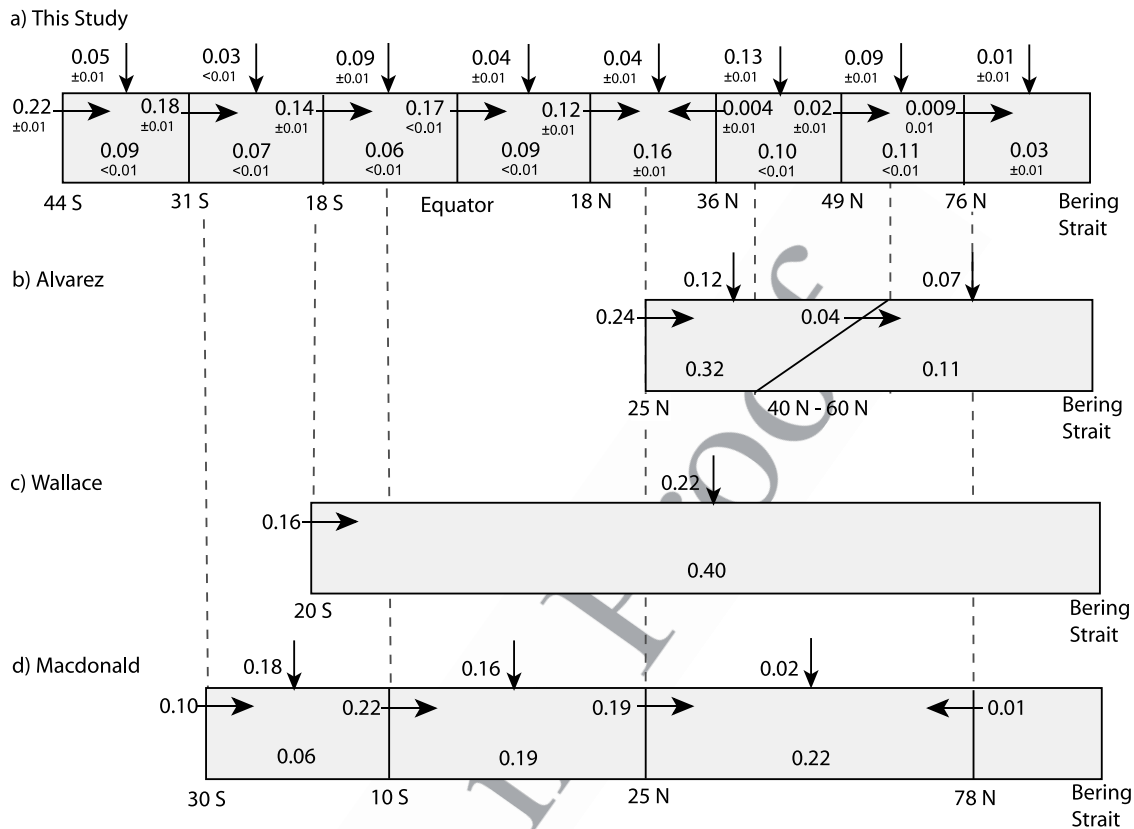
Figure 5. Uptake, storage, and transport of anthropogenic CO_2 in the Atlantic Ocean (Pg C yr^{-1}) based on (a) this study (weighted mean and standard deviation scaled to 1995), (b) the estimates of [*Álvarez et al.*, 2003], where the transport across 24°N was taken from *Rosón et al.* [2003], (c) *Wallace* [2001], where the transport across 20°S was taken from *Holfort et al.* [1998], and (d) *Macdonald et al.* [2003], where the transports across 10°S and 30°S were taken from *Holfort et al.* [1998], and the transport across 78°N was taken from *Lundberg and Haugan* [1996]. This figure is not to scale.

auxiliary material, regions 25 and 30). Since this transport exceeds storage in the South Pacific, it drives equatorward transport of anthropogenic CO_2 throughout the South Pacific and substantial northward cross-equatorial transport (Figure 4). In the North Pacific, the greatest anthropogenic CO_2 uptake occurs at high latitudes and in the tropics. Anthropogenic CO_2 taken up in the North Pacific is transported equatorward (Figure fs02 of the auxiliary material, regions 11 and 12), and anthropogenic CO_2 from the tropics is transported poleward (Figure fs02 of the auxiliary material, regions 16 and 17), leading to convergence and storage in the subtropical North Pacific.

[30] The Indonesian throughflow plays a critical role in determining the transports in the Indian and Pacific oceans south of 18°N (Figure 4) as it sets up a transport loop that involves strong northward transport in the South Pacific and southward transport in the southern Indian Ocean. We computed the anthropogenic CO_2 transport by the Indonesian throughflow for each model by multiplying at each model depth the diagnosed volume flux in the model with the anthropogenic CO_2 concentration estimate from the GLODAP gridded data set, interpolated to the throughflow point in each model. The OGCM simulated volume fluxes across the straight are generally within the range of obser-

vational estimates [e.g., *Gordon and Fine*, 1996], but these estimates are themselves rather uncertain since this transport is not well understood and may have significant interannual variability. We therefore regard our estimated time-integrated transport of 10.6 ± 0.5 Pg C by the Indonesian throughflow as an uncertain component of our transport estimates.

[31] In Figure 5, we compare our transport estimates for the Atlantic with those estimated from hydrographic data and data-based anthropogenic CO_2 estimates [e.g., *Lundberg and Haugan*, 1996; *Holfort et al.*, 1998; *Álvarez et al.*, 2003; *Rosón et al.*, 2003; *Macdonald et al.*, 2003]. This comparison remains somewhat qualitative, as these hydrographic estimates are subject to substantial uncertainties from a variety of factors [e.g., *Macdonald et al.*, 2003]. In addition, the hydrographic data-based estimates determine the transport at a single point in time and could be substantially biased owing to the neglect of seasonal variations in transport [e.g., *Wilkin et al.*, 1995]. In contrast, our estimate of the anthropogenic CO_2 transport is scaled from the time-integrated transport from 1765 to 1995, and reflects a long-term mean transport. Therefore, even if the hydrographic data-based estimates were insensitive to seasonal biases, the two transports are not directly comparable as they pertain to very different time periods. In addition, there

are sources of uncertainty associated with the inverse estimates that have not been quantified, as discussed in section 4. These caveats need to be considered when comparing the results.

[32] In order to arrive at transport estimates for a particular year, we scaled the time integrated transports to 1995 using the atmospheric perturbation. We assumed inventory in each region increases proportionally with the perturbation to atmospheric CO_2, such that the regional transports scale proportionally. This scaling is supported by an analysis of forward model simulations (Figure fs08 of the auxiliary material).

[33] Both our estimates and hydrographic transects find substantial northward transport throughout the South Atlantic (Figure 5). Our transport estimate across 31°S is 70% larger than the estimate of 0.1 ± 0.02 Pg C yr^{-1} across 30°S determined by *Holfort et al.* [1998]. However, our estimate of 0.14 ± 0.01 Pg C yr^{-1} northward transport across 18°S is in reasonable agreement with *Wallace* [2001], who found 0.16 ± 0.02 Pg C yr^{-1} northward transport across 20°S.

[34] In the North Atlantic, we find a northward transport of 0.12 ± 0.01 Pg C yr^{-1} across 18°N and no significant transport across 36°N. This is substantially smaller than the northward transport of 0.24 ± 0.08 Pg C yr^{-1} and 0.19 ± 0.08 Pg C yr^{-1} across 25°N estimated by *Rosón et al.* [2003] and *Macdonald et al.* [2003], respectively. However, owing to the large uncertainties associated with the hydrographic estimates, the differences are only marginally statistically significant. We find a small northward transport across 49°N of 0.02 ± 0.01 Pg C yr^{-1} that is in good agreement with the transport estimated across a diagonal transect between 40°N and 60°N [*Álvarez et al.*, 2003]. Finally, we find a marginally significant northward transport at 76°N, whereas *Lundberg and Haugan* [1996] estimated a southward transport at 78°N. The small northward transport across 76°N is very sensitive to the choice of OGCM, as will be shown in the following section. Therefore we conclude that our northward transport at 76°N is not a robust result of the inversion, while the transports at the more southern latitudes in the Atlantic are found to be generally invariant across the models investigated.

4. Sensitivity and Error Analysis

[35] In this section, we address and quantify two sources of error in the inversion. First, we use basis functions from 10 OGCMs to assess the sensitivity of the estimates to the choice of transport model. Then we address the sensitivity of the inversion to biases in the data-based estimates of the anthropogenic CO_2 concentrations.

[36] There are other potential sources of error that will not be addressed here. The most important is our assumption that the ocean circulation has remained constant over time. There is substantial evidence for decadal variability in ocean circulation from repeat hydrography studies [e.g., *García et al.*, 2002; *Bryden et al.*, 2003; *Johnson and Gruber*, 2006; *McPhaden and Zhang*, 2002], which could lead to biases in the inverse estimates. For example, if the ventilation in a given region were weakening progressively over time, a basis function generated for that region using constant present-day circulation would underestimate the fraction of dye near the surface relative to the portion of dye in deeper waters. We are currently unable to quantitatively assess the possible impact of long-term changes in ocean circulation on our inverse results. Forward simulations by *Raynaud et al.* [2005] suggest that variations in ocean circulation have a relatively small impact on the air-sea flux of anthropogenic CO_2 on interannual timescales, but may be more substantial on decadal timescales. However, comparisons between simulations of CFCs with constant circulation and observations do not indicate major problems as a result of decadal variability [*Dutay et al.*, 2002].

[37] There are also potential methodological sources of errors. For example, the relatively small number of model regions used here may cause aggregation errors [*Kaminski et al.*, 2001]. However, on the basis of the analysis of the covariance matrix (see text01 section of the auxiliary material), we conclude that a larger number of model regions is likely to yield a solution that is not adequately constrained by the observations. A second issue is the spatial and temporal pattern used to prescribe the distribution of the fluxes within the model region. Inverse estimates using several different spatial patterns indicate that the flux estimates are not particularly sensitive to the choice of spatial pattern or whether the pattern includes seasonal variations [*Gloor et al.*, 2001].

4.1. Sensitivity to the Choice of OGCM

[38] On the basis of a comparison of the 10 OGCMs considered in this study, we find that most of the major features of the spatial pattern of the anthropogenic CO_2 uptake and transport estimates are generally robust. However, there are substantial between-model differences in some regions.

[39] The largest variability differences between models occurs in the Southern Ocean (see Figures fs03, fs06, and fs09 in the auxiliary material) as found by OCMIP\-2 [*Orr et al.*, 2001; *Watson and Orr*, 2003; *Doney et al.*, 2004]. *Doney et al.* [2004] cite limitations of the models in accurately representing along-isopycnal transport, brine rejection due to sea ice formation, boundary conditions, the role of eddies and how they are parameterized, and the lack of data available to validate the models in this region as the major reasons for this large spread in model behavior. In our inversion, the UL and MIT models give the largest anthropogenic CO_2 uptake and storage in the Southern Ocean. The UL model has the poorest CFC skill score, but the MIT skill score is close to the average of all models used here. These two models entrain a larger portion of the anthropogenic CO_2 injected between 44°S and 58°S into deep waters and transport a smaller portion to the midlatitudes than all of the other models (see, for example, basis functions for the subpolar Atlantic in Figures fs06 and fs07 of the auxiliary material). The midlatitude basis functions have relatively shallow dye penetration. Therefore a greater anthropogenic CO_2 uptake is required at high latitudes to match the observed storage in midlatitude intermediate waters.

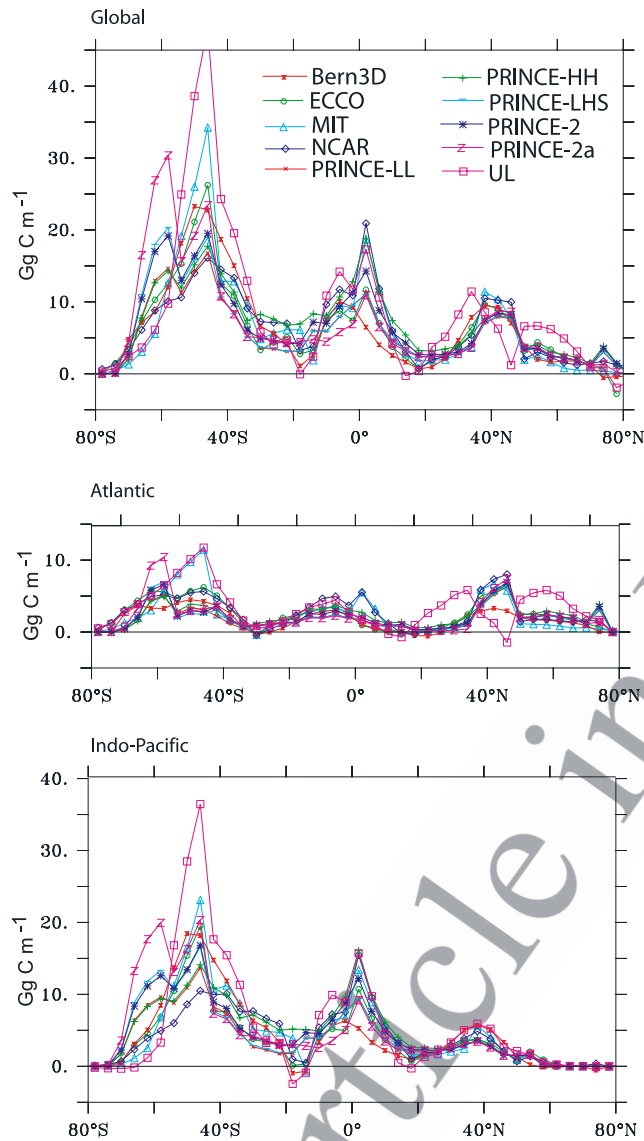[40] The Arctic Ocean is the second region showing high between-model differences in the estimated fluxes. This is

Figure 6. Zonally and temporally integrated anthropogenic CO_2 uptake by (top) the global ocean, (middle) the Atlantic Ocean, and (bottom) the Indo-Pacific Ocean from 1765–1995.

likely due to the large differences between models in the representation of this basin. Some models have a well-resolved Arctic basin due to their shifting the North Pole over land; others do not resolve it at all. We therefore have little confidence in the estimated fluxes for this basin. Fortunately, this has little influence on our results, as the fluxes are expected to be small owing to sea-ice inhibiting the uptake for a large portion of the Arctic.

[41] The inverse estimates for most of the OGCMs used in this study are in excellent agreement in the Atlantic. However, the UL model exhibits a different latitudinal distribution of anthropogenic CO_2 uptake (Figure 6). This can be traced back to this model storing a large portion of the dye tracer injected into the high-latitude North Atlantic near the surface. As discussed further in the auxiliary

material, this leads to a rearrangement of the flux distribution in order to match the data-based estimates of anthropogenic CO_2.

[42] One way to evaluate the different models and to assess biases in the inverse estimates is to examine the residuals between the data-based anthropogenic CO_2 estimates and the anthropogenic CO_2 storage calculated from the inverse flux estimates (Figure 7). The models underestimate the mean anthropogenic CO_2 concentration by about 1 to 2.5 μmol kg^{-1}. In addition, all of the models underestimate anthropogenic CO_2 storage in the thermocline (500 to 1000 m). This suggests that they either do not sufficiently ventilate this region, or that the anthropogenic CO_2 estimates in this region are biased high. As discussed in more detail in the following section, this region has not been identified as a region of substantial possible biases in the data-based estimates of anthropogenic CO_2 [*Matsumoto and Gruber*, 2005], so that an overly weak ventilation in the models is the more likely cause of the positive residuals in the deeper thermocline.

[43] In waters shallower than 500 m, most of the models show negative residuals at around 20°N and 30°S and positive residuals in the tropics and at around 40°N and 40°S. One possible explanation for this structure is that the models have excessive poleward transport out of the tropics and too strong equatorward transport out of the high latitudes. If this were the case, the uptake might be overestimated in the tropics and at high latitudes in order to match the substantial anthropogenic CO_2 concentrations in these areas. A large portion of this excessive flux would then be transported to midlatitudes, leading to an overestimate of the anthropogenic CO_2 storage. An alternative explanation is a bias in the reconstructed anthropogenic CO_2 concentrations. *Matsumoto and Gruber* [2005] showed that the ΔC^* method tends to be biased high in the upper thermocline, explaining at least part of the positive residuals in this region.

[44] In the Southern Ocean, most of the models have negative residuals between about 200 m and 1000 m and positive residuals in the deep waters. If the data-based estimates of anthropogenic CO_2 were correct, this would suggest that the models tend to overestimate the vertical transport of anthropogenic CO_2 in the upper 1000 m of the Southern Ocean and that they are unable to represent the small anthropogenic CO_2 concentrations found in the deep Southern Ocean. Since the identified possible biases in the data-based estimates of anthropogenic CO_2 are an overestimation in the upper ocean and an underestimation in the deep ocean [*Matsumoto and Gruber*, 2005], the adjustment for this possible error in anthropogenic CO_2 would actually accentuate the residuals rather than ameliorate them. This points to a persistent problem in the employed OGCMs in how they simulate the circulation in the Southern Ocean. The UL and PRINCE-LL models, which have the lowest CFC-11 skill scores (Table 1), represent the two extreme cases. The UL model, which finds substantially more anthropogenic CO_2 uptake than any of the other contributing models, has large negative residuals throughout most of the Southern Ocean, suggesting that its inversely estimated uptake is too large. In contrast, the PRINCE-LL model,
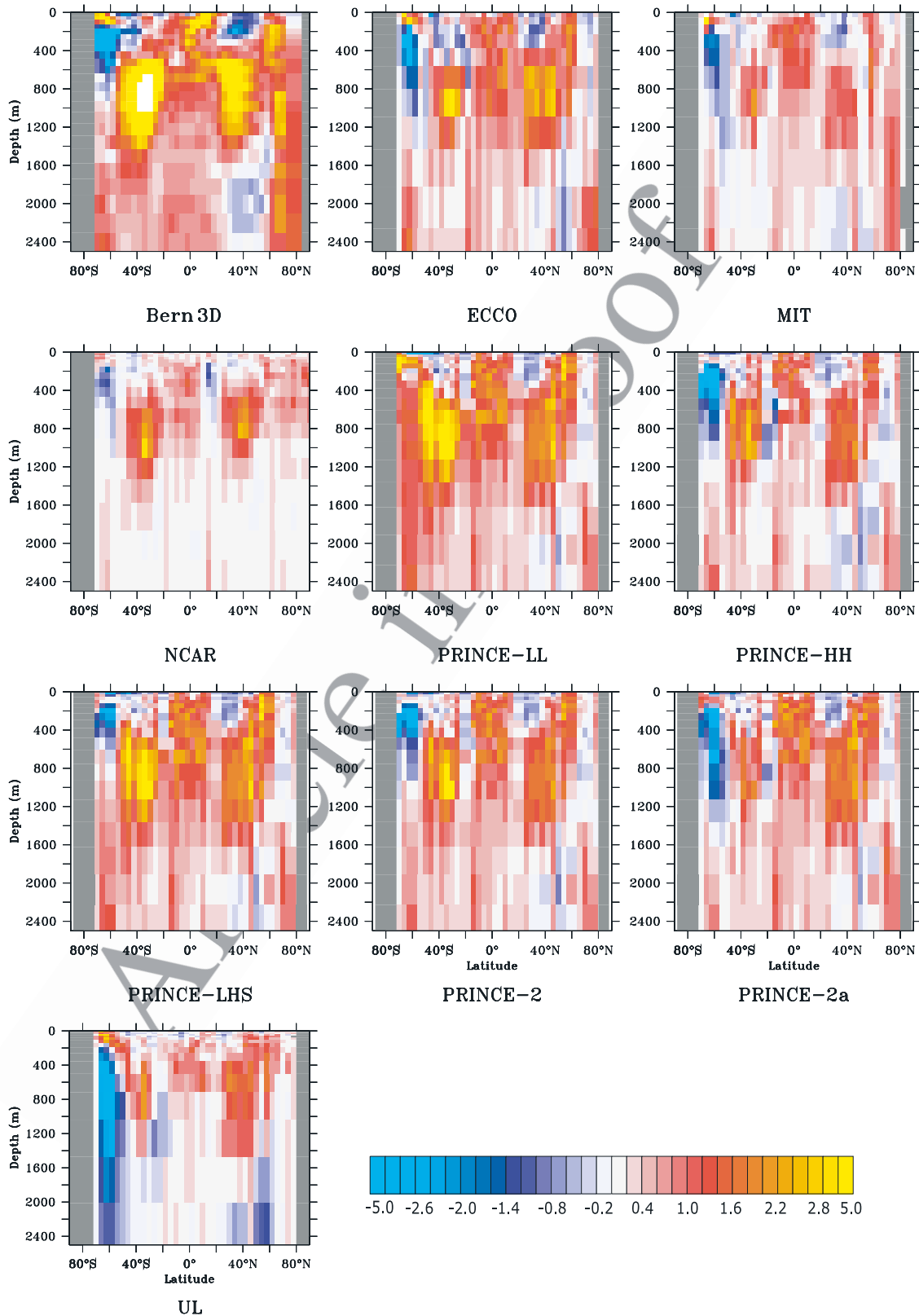
Figure 7. Meridional section of the zonal mean of the difference between the data-based anthropogenic CO_2 estimates and the inverse anthropogenic CO_2 storage estimates (μmol kg^{-1}) for the 10 models that participated in this study. Solid gray areas represent locations where no observations are available or that are outside the model grid. Little spatial structure to the residuals exists below 2500 m.

which has the lowest global anthropogenic CO_2 uptake, has positive residuals throughout the Southern Ocean. This model is characterized by very low vertical and along-isopycnal diffusivity, so that a much greater portion of the anthropogenic CO_2 remains near the surface. The resulting underestimation of the data-based estimates points to this model being deficient in its uptake. Thus the large residuals exhibited by these two models confirm their having a low CFC-11 skill score. Their large residuals also confirm our use of these skill scores as weights for computing means and standard deviations, as the likelihood of these two models being accurate is smaller than that of the other models.

4.2. Sensitivity to Errors in the Anthropogenic CO_2 Estimates

[45] Inverse estimates rest on the assumption that the observations used to constrain the inversion are accurate. However, we constrain our inversion with an estimated quantity, which may contain biases. This makes it necessary to test the sensitivity of the inverse flux estimates to such biases. First, we examine the impact of a density-dependent bias modeled after that identified by *Matsumoto and Gruber* [2005]. Then we investigate the effect of biases in the stoichiometric ratios used to remove the effects of biology from the observed CO_2 concentration. *Gruber* [1998] argued that biases in this ratio could substantially alter the distribution of anthropogenic CO_2 as well as the total inventory.

[46] We will not investigate the impact of possible biases in anthropogenic CO_2 emerging from the fact that possible changes in ocean circulation due to ocean warming were not taken into account in estimating the anthropogenic CO_2 inventory [*Keeling*, 2005]. *Matsumoto and Gruber* [2005] showed, however, that changes in ocean circulation and biogeochemistry have relatively little impact on the estimated anthropogenic CO_2 concentrations [see also *Sabine and Gruber*, 2005].

[47] *Matsumoto and Gruber* [2005] examined the accuracy of the anthropogenic CO_2 estimates by applying the ΔC^* method to results from a forward model simulation with known anthropogenic CO_2 concentrations. The authors identified substantial biases in the ΔC^* method stemming from the neglected time evolution of the air-sea disequilibrium, biases in the *p*CFC ventilation age, and errors in identifying water masses that contribute to a given water parcel. As a result, they suggested that the ΔC^* method tends to overestimate the anthropogenic CO_2 inventory in shallower waters by about 10% and underestimate it in deeper waters. Globally, the ΔC^* method inferred anthropogenic CO_2 inventory was about 7% larger than the true inventory.

[48] It is not within the scope of this paper to reassess the anthropogenic CO_2 data set based on the findings of *Matsumoto and Gruber* [2005]. However, it is critical to address the impact these biases might have on the inverse estimates. To this end, we constructed a "Matsumoto and Gruber corrected" scenario, in which a hypothetical correction factor was applied to the data-based anthropogenic CO_2 estimates and these corrected anthropogenic CO_2 estimates were used in the inversion. The correction factor was determined as a function of density in such a way that it reduced anthropogenic CO_2 in the upper ocean by about 10% and increased it in the deep ocean slightly, while reducing the global inventory by 7%. In addition, two scenarios were constructed to assess the impact of a globally uniform shift in the oxygen to carbon remineralization ratio, $r_{C:O_2}$, used to remove the effects of biology. The construction of these scenarios is described in section 4 of the text01 file in the auxiliary material.

[49] The spatial pattern of the inversely estimated air-sea fluxes is remarkably insensitive to these biases (Figure 8); however, the net global anthropogenic CO_2 uptake scales approximately linearly with changes in the estimated global inventory of anthropogenic CO_2 (8, numerical results shown in Table ts04 of the auxiliary material). The Matsumoto and Gruber scenario leads to a global reduction in the anthropogenic CO_2 uptake of 8%, reflecting the global 7% decrease in the anthropogenic CO_2 inventory. Relative to the global uptake, the anthropogenic uptake at high latitudes (north of 49°N and south of 58°S) is increased slightly and the uptake in all other regions is decreased slightly by the hypothetical correction. Increasing the stoichiometric ratio, $r_{C:O_2}$, by 13% decreases the global anthropogenic CO_2 flux by 7%, and decreasing $r_{C:O_2}$ by 13% increases the global flux by 8%. In the ΔC^* method, $r_{C:O_2}$ together with AOU is used to subtract the effect of changes in DIC as a result of biological processes. Therefore increases in $r_{C:O_2}$ are expected to lead to decreases in the estimated anthropogenic CO_2, and vice versa. The inverse estimates are least sensitive to changes in $r_{C:O_2}$ at midlatitudes, where AOU is lowest, and most sensitive at high latitudes and in the tropical Pacific.

[50] We conclude from these analyses that the inverse flux estimates generally tend to be more sensitive to the choice of model than to biases in the anthropogenic CO_2 estimates. Therefore, despite the fact we employed 10 different OGCMs and used CFC skill scores to weight the different models, possible biases in model transport still tends to dominate the overall uncertainty in our flux estimates.

5. Comparison of Forward and Inverse Models

[51] Traditionally, the spatial distribution of the air-sea flux of anthropogenic CO_2 has been estimated using forward simulations of OGCMs forced by the observed atmospheric CO_2 perturbation [e.g., *Orr et al.*, 2001; *Murnane et al.*, 1999; *Sarmiento et al.*, 1992]. In this section, the inverse estimates of each OGCM are compared with their corresponding forward estimates undertaken as part of OCMIP-2 [*Watson and Orr*, 2003] in order to assess what we have learned by constraining the models with the data-based anthropogenic CO_2 estimates.

[52] The difference between the forward simulations and the corresponding inverse estimates of anthropogenic CO_2 for 1995 from seven of the ten models used in this study are shown in Figure 9 (complete numerical results shown in Table ts05 of the auxiliary material). Positive values indicate that the forward model simulates more anthropogenic CO_2 uptake than the inversion and vice versa. The Bern3D,
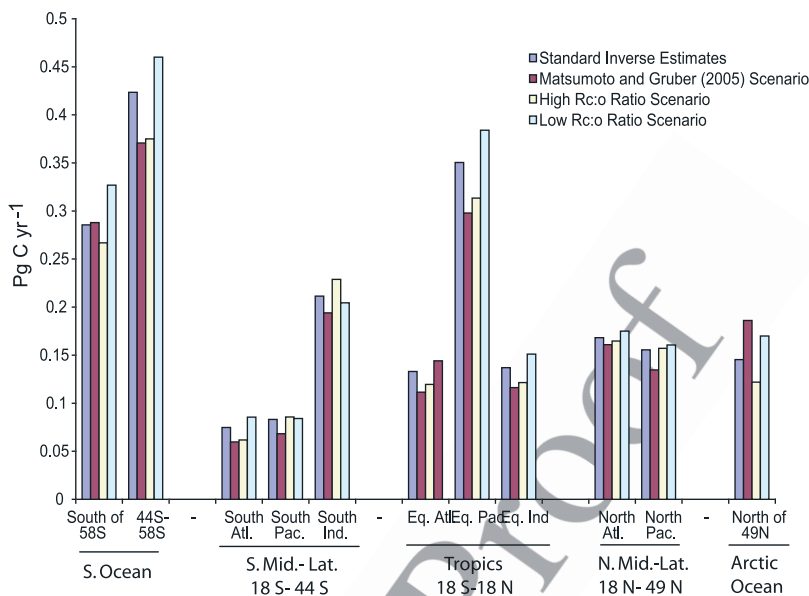
Figure 8. Sensitivity of the inverse estimates of the anthropogenic CO_2 fluxes (Pg C yr^{-1}, scaled to 1995) to errors in the data-based anthropogenic CO_2 estimates used to constrain the inversion. The anthropogenic CO_2 fluxes have been estimated using the standard data-based anthropogenic CO_2 estimates from GLODAP, anthropogenic CO_2 estimates with a hypothetical correction based on work by *Matsumoto and Gruber* [2005], and anthropogenic estimates based on the high and low end of the range associated with the CO_2 to oxygen ratio [*Anderson and Sarmiento*, 1994]. The inverse estimates are aggregated to 11 regions for clarity.
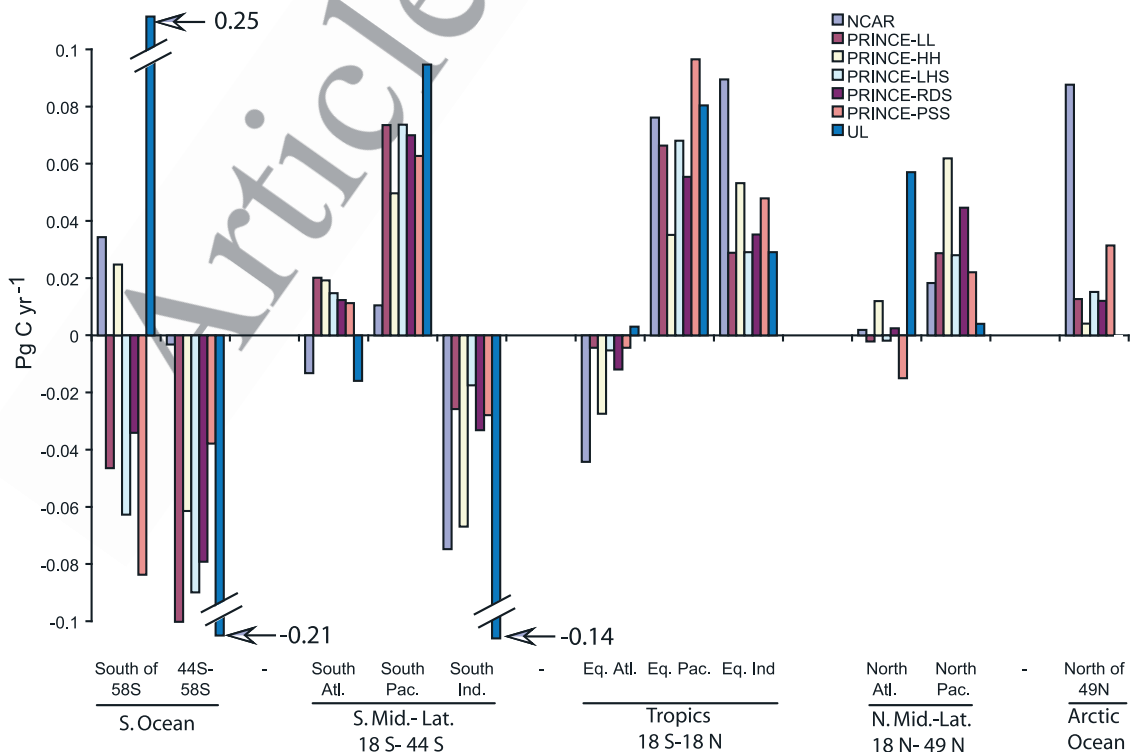

Figure 9. Zonally integrated difference between the forward and inverse anthropogenic CO_2 uptake estimates for 1995 (a positive value indicate that the forward uptake flux is larger than the inverse). Forward simulations are from OCMIP-2 [*Watson and Orr*, 2003]. Positive (negative) values indicate that the forward simulation finds more (less) anthropogenic CO_2 uptake than the inversion.

ECCO, and MIT models are not included because their forward simulations were not available at the time of this writing.

[53] There are clearly trends in the difference between the forward and inverse estimates across all models (Figure 9). The forward model simulations for those models included both in this study and in OCMIP-2 find a global anthropogenic CO_2 uptake of 2.3 ± 0.32 Pg C yr^{-1} when the mean and standard deviation are weighted in the same way as the inverse estimates. In comparison, the inverse estimates find 0.1 Pg C yr^{-1} less uptake than the forward simulations and reduce the uncertainty estimate by 22%. For most of the models, the inverse anthropogenic CO_2 uptake estimates are substantially larger than those of the forward model estimates in the Southern Ocean between 44°S and 58°S and in the Indian Ocean south of 18°S. This is primarily driven by all of the forward models simulating a smaller anthropogenic CO_2 storage in the midlatitudes of the Southern Hemisphere, particularly in the Indo-Pacific (Figure fs11 of the auxiliary material). In order to match the data-based estimates, the inversion requires a more vigorous flux into the subpolar South Atlantic and subpolar Indo-Pacific, whose signal is then transported equatorward to midlatitudes. An exception to this pattern is the NCAR model, for which the inversion finds a smaller anthropogenic CO_2 uptake in these regions compared to the forward simulations. However, in southern midlatitudes, where most of the inverse models show decreased uptake compared to the forward models, the NCAR model finds increased anthropogenic CO_2 uptake in the Atlantic and only slightly decreased anthropogenic CO_2 uptake in the Pacific. This suggests that fluxes from these regions contribute strongly to matching the observed midlatitude storage in the NCAR inversion. The other large exception is the UL model, for which the inversion suggests a strong equatorward shift of uptake, away from the high latitudes in the Southern Ocean.

[54] In the Atlantic, most of the models find more anthropogenic uptake than the forward models around 40°N and from 18°S to the equator (Figure 9). The inversion generally finds less anthropogenic CO_2 uptake from 18°N to 36°N and at high northern latitudes.

[55] These consistent differences between the forward and inverse estimates suggest that using the data-based anthropogenic CO_2 estimates to constrain the flux estimates adds new, quantitative information about the spatial distribution of the anthropogenic CO_2 fluxes that cannot be gained using OGCMs alone. There are three possible causes for differences between the forward estimates and the inverse estimates. Differences could be a result of deficiencies in the model's underlying physical circulation. There could be large-scale biases in the data-based anthropogenic CO_2 estimates used to constrain the inversion; however, the spatial pattern of the inverse flux estimates have been shown to be insensitive to several potential biases in the ΔC^* method. Finally, there may be errors in the air-sea gas exchange in the forward models.

6. Conclusions

[56] The Green's function inverse approach presented here is currently the only method that has been applied globally to estimate the air-sea flux of anthropogenic CO_2 from data-based estimates of its ocean interior distribution. A related tracer-based method, the transit time distribution method, has recently been developed to do this as well [*Hall and Primeau*, 2004], but it has not yet been applied globally. Other promising methods include the adjoint method [*Schlitzer*, 2004], but this approach has not been applied to estimating air-sea fluxes of anthropogenic CO_2.

[57] A previous inversion study employing the same Green's function technique suggested that while the uncertainty of the inversely estimated fluxes due to random errors is remarkably small, substantial potential for bias exists because of the uncertainty in the OGCMs used to represent ocean transport and mixing [*Gloor et al.*, 2001]. Our investigation using a suite of ten OGCMs suggests that the inversely estimated fluxes of anthropogenic CO_2 are generally insensitive to potential biases introduced by OGCM transport and mixing. This is not the case for all regions, though, as substantial uncertainties persist in a few of them, particularly in the Southern Ocean. We also find that the spatial pattern of the air-sea fluxes is remarkably robust with respect to three scenarios for biases in the data-based estimates of anthropogenic CO_2, but the net global uptake flux scales approximately linearly with changes in the global anthropogenic CO_2 inventory. We did not investigate the potential impact of long-term changes in ocean circulation and biogeochemistry on our inversion results, but on the basis of our current understanding we believe that this impact has remained small so far. Given the near-exponential growth of atmospheric CO_2 and radiative forcing, we expect this impact to grow with time, however. This will require the development of new methods to determine the anthropogenic CO_2, as well as the use of time varying circulation models in order to use this method in the future.

[58] On the basis of our relatively broad investigation of errors and biases in data and models, we conclude that our best estimate for the oceanic uptake rate of anthropogenic CO_2 for a nominal year of 1995 is 2.2 Pg C yr^{-1}, with an uncertainty due to errors in OGCM transport of ±0.25 Pg C yr^{-1} (1-sigma). This represents a 22% improvement in error estimates over forward simulations when the same method is used to weight the standard deviation of the models. We estimate that the uncertainty due to potential biases in the data-based estimates is somewhat smaller than the uncertainty due to errors in OGCM transport. The ocean inversion provides strong constraints for the global budget of anthropogenic CO_2, in particular the net uptake by the terrestrial biosphere (see A. R. Jacobson et al., A joint atmosphere-ocean inversion for surface fluxes of carbon dioxide: 2. Results, submitted to *Global Biogeochemical Cycles*, 2006).

936 tion (OCE-0137274). Climate and Environmental Physics, Bern acknowl-
937 edges support by the European Union through the Integrated Project
938 CarboOcean and the Swiss National Science Foundation.

References

940 Álvarez, M., A. Ríos, F. F. Pérez, H. L. Bryden, and G. Rosón (2003),
941 Transports and budgets of total inorganic carbon in the subpolar and
942 temperate North Atlantic, *Global Biogeochem. Cycles*, *17*(1), 1002,
943 doi:10.1029/2002GB001881.
944 Anderson, L. A., and J. L. Sarmiento (1994), Redfield ratios of reminer-
945 alization determined by nutrient data analysis, *Global Biogeochem. Cy-
946 cles*, *8*(1), 65–80.
947 Bousquet, P., P. Peylin, P. Ciais, C. LeQuéré, P. Friedlingstein, and P. P.
948 Tans (2000), Regional changes in carbon dioxide fluxes of land and
949 oceans since 1980, *Science*, *290*, 1342–1346.
950 Bryden, H. L., E. L. McDonagh, and B. A. King (2003), Changes in ocean
951 water mass properties: Oscillations or trends?, *Science*, *300*, 2086–2088.
952 Doney, S., et al. (2004), Evaluating global ocean carbon models: The im-
953 portance of realistic physics, *Global Biogeochem. Cycles*, *18*, GB3017,
954 doi:10.1029/2003GB002150.
955 Dutay, J.-C., et al. (2002), Evaluation of ocean model ventilation with CFC-
956 11: Comparison of 13 global ocean models, *Ocean Modell.*, *4*, 89–120.
957 Enting, I. G., and J. V. Mansbridge (1989), Latitudinal distribution of
958 sources and sinks of atmospheric CO_2: Direct inversion of filtered data,
959 *Tellus, Ser. B.*, *41*, 111–126.
960 Enting, I. G., T. M. L. Wigley, and M. Heimann (1994), Future emissions
961 and concentrations of carbon dioxide: Key ocean/atmosphere/land ana-
962 lyses, technical report, Div. of Atmos. Res., Comonw. Sci. and Ind. Res.
963 Org., Melbourne, Australia.
964 Etheridge, D. M., L. P. Steele, R. L. Langenfelds, R. J. Francey, J.-M.
965 Barnola, and V. I. Morgan (1996), Natural and anthropogenic changes
966 in atmospheric CO_2 over the last 1000 years from air in Antarctic ice and
967 firn, *J. Geophys. Res.*, *101*(D2), 4115–4128.
968 Friedli, H., H. Loetscher, H. Oeschger, U. Siegenthaler, and B. Stauffer
969 (1986), Ice core record of the $^{13}C/^{12}C$ ratio of atmospheric CO_2 in the
970 past two centuries, *Nature*, *324*, 237–238.
971 García, M., I. Bladé, A. Cruzado, Z. Velásquez, H. García,
972 J. Puigdefabregas, and J. Sospedra (2002), Observed variability of water
973 properties and transports on the World Ocean Circulation Experiment
974 SR1b section across the Antarctic Circumpolar Current, *J. Geophys.
975 Res.*, *107*(C10), 3162, doi:10.1029/2000JC000277.
976 Gloor, M., N. Gruber, T. M. C. Hughes, and J. L. Sarmiento (2001), An
977 inverse modeling method for estimation of net air-sea fluxes from bulk
978 data: Methodology and application to the heat cycle, *Global Biogeochem.
979 Cycles*, *15*(4), 767–782.
980 Gloor, M., N. Gruber, J. L. Sarmiento, C. L. Sabine, R. A. Feely, and
981 C. Roedenbeck (2003), A first estimate of present and pre-industrial
982 air-sea CO_2 fluxes patterns based on ocean interior carbon measurements
983 and models, *Geophys. Res. Lett.*, *30*(1), 1010, doi:10.1029/
984 2002GL015594.
985 Gnanadesikan, A., N. Gruber, R. D. Slater, and J. L. Sarmiento (2002),
986 Oceanic vertical exchange and new production: A comparison between
987 model results and observations, *Deep Sea Res., Part II*, *49*, 363–401.
988 Gnanadesikan, A., J. P. Dunne, R. M. Key, K. Matsumoto, J. L. Sarmiento,
989 R. D. Slater, and P. S. Swathi (2004), Oceanic ventilation and biogeo-
990 chemical cycling: Understanding the physical mechanisms that produce
991 realistic distributions of tracers and productivity, *Global Biogeochem.
992 Cycles*, *18*, GB4010, doi:10.1029/2003GB002097.
993 Gordon, A. L., and R. A. Fine (1996), Pathways of water between the
994 Pacific and Indian Oceans in the Indonesian Seas, *Nature*, *379*, 146–149.
995 Gruber, N. (1998), Anthropogenic CO_2 in the Atlantic Ocean, *Global Bio-
996 geochem. Cycles*, *12*(1), 165–191.
997 Gruber, N., J. L. Sarmiento, and T. F. Stocker (1996), An improved method
998 for detecting anthropogenic CO_2 in the oceans, *Global Biogeochem.
999 Cycles*, *10*(4), 809–837.
1000 Gruber, N., M. Gloor, T. M. C. Hughes, and J. L. Sarmiento (2001), Air-sea
1001 flux of oxygen estimated from bulk data: Implications for the marine and
1002 atmospheric oxygen cycle, *Global Biogeochem. Cycles*, *15*(4), 783–803.
1003 Gruber, N., C. D. Keeling, and N. R. Bates (2002), Interannual variability in
1004 the North Atlantic Ocean carbon sink, *Science*, *298*, 2374–2378.
1005 Hall, T. M., and F. W. Primeau (2004), Separating the natural and anthro-
1006 pogenic air-sea flux of CO_2: The Indian Ocean, *Geophys. Res. Lett.*, *31*,
1007 L23302, doi:10.1029/2004GL020589.
1008 Holfort, J., K. M. Johnson, B. Siedler, and D. W. R. Wallace (1998),
1009 Meridional transport of dissolved inorganic carbon in the South Atlantic
1010 Ocean, *Global Biogeochem. Cycles*, *12*(3), 479–499.
1011 Johnson, G. C., and N. Gruber (2006), Decadal water mass variations along
1012 20°W in the northeastern Atlantic Ocean, *Prog. Oceanogr.*, in press.

1013 Kaminski, T., P. J. Rayner, M. Heimann, and I. G. Enting (2001), On
1014 aggregation errors in atmospheric transport inversions, *J. Geophys.
1015 Res.*, *106*(D5), 4703–4716.
1016 Keeling, R. F. (2005), Comment on "The ocean sink for atmospheric CO_2,"
1017 *Science*, *381*, 1734, doi:10.1126/science.1109620.
1018 Keeling, C. D., R. B. Bacastow, A. F. Carter, S. C. Piper, T. P. Whorf,
1019 M. Heimann, W. G. Mook, and H. Roeloffzen (1989), A three-dimen-
1020 sional model of atmospheric CO_2 transport based on observed winds: 1.
1021 Analysis of observational data, in *Aspects of Climate Variability in the
1022 Pacific and the Western Americas, Geophys. Monogr. Ser.*, vol. 55, edited
1023 by D. H. Peterson, pp. 165–237, AGU, Washington, D. C.
1024 Keeling, C. D., H. Brix, and N. Gruber (2004), Seasonal and long-term
1025 dynamics of the upper ocean carbon cycle at station ALOHA near Ha-
1026 waii, *Global Biogeochem. Cycles*, *18*, GB4006, doi:10.1029/
1027 2004GB002227.
1028 Key, R. M., A. Kozyr, C. L. Sabine, K. Lee, R. Wanninkhof, J. L. Bullister,
1029 R. A. Feely, F. J. Millero, C. Mordy, and T.-H. Peng (2004), A global
1030 ocean carbon climatology: Results from Global Data Analysis Project
1031 (GLODAP), *Global Biogeochem. Cycles*, *18*, GB4031, doi:10.1029/
1032 2004GB002247.
1033 Lee, K., et al. (2003), An updated anthropogenic CO_2 inventory in the
1034 Atlantic Ocean, *Global Biogeochem. Cycles*, *17*(4), 1116, doi:10.1029/
1035 2003GB002067.
1036 Lundberg, L., and P. M. Haugan (1996), A nordic seas–Arctic Ocean
1037 carbon budget from volume flows and inorganic carbon data, *Global
1038 Biogeochem. Cycles*, *10*(3), 493–510.
1039 Macdonald, A. M., M. O. Baringer, R. Wanninkhof, K. Lee, and D. W. R.
1040 Wallace (2003), A 1998–1992 comparison of inorganic carbon and its
1041 transport across 24.5°N in the Atlantic, *Deep Sea Res., Part II*, *50*, 3041–
1042 3064.
1043 Maier-Reimer, E., and K. Hasselmann (1987), Transport and storage of CO_2
1044 in the ocean—An inorganic ocean-circulation carbon cycle model, *Clim.
1045 Dyn.*, *2*, 63–90.
1046 Matsumoto, K., and N. Gruber (2005), How accurate is the estimation of
1047 anthropogenic carbon in the ocean: An evaluation of the ΔC^* method,
1048 *Global Biogeochem. Cycles*, *19*, GB3014, doi:10.1029/2004GB002397.
1049 Matsumoto, K., et al. (2004), Evaluation of ocean carbon cycle models with
1050 data-based metrics, *Geophys. Res. Lett.*, *31*, L07303, doi:10.1029/
1051 2003GL018970.
1052 McPhaden, M. J., and D. Zhang (2002), Slowdown of the meridional over-
1053 turning circulation in the upper Pacific Ocean, *Nature*, *415*, 603–608.
1054 Mikaloff Fletcher, S. E., N. P. Gruber, and A. Jacobson (2003), Ocean
1055 Inversion Project how-to document, version 1.0, report, 18 pp., Inst.
1056 for Geophys. and Planet. Phys., Univ. of Calif., Los Angeles.
1057 Murnane, R. J., J. L. Sarmiento, and C. LeQuéré (1999), Spatial distribution
1058 of air-sea fluxes and the interhemispheric transport of carbon by the
1059 oceans, *Global Biogeochem. Cycles*, *13*(2), 287–305.
1060 Neftel, A., E. Moor, H. Oeschger, and B. Stauffer (1985), Evidence from
1061 polar ice cores for the increase in atmospheric CO2 in the past two
1062 centuries, *Nature*, *315*, 45–47.
1063 Orr, J. C., et al. (2001), Estimates of anthropogenic carbon uptake from four
1064 three-dimensional global ocean models, *Global Biogeochem. Cycles*,
1065 *15*(1), 43–60.
1066 Raynaud, S., O. Aumont, K. Rodgers, P. Yiou, and J. C. Orr (2005), Inter-
1067 annual-to-decadal variability of North Atlantic air-sea CO_2 fluxes, *Ocean
1068 Sci. Discuss.*, *2*, 437–472.
1069 Rosón, G., A. F. Ríos, F. F. Pérez, A. Lavin, and H. L. Bryden (2003),
1070 Carbon distribution, fluxes, and budgets in the subtropical North Atlantic
1071 Ocean (24.5°N), *J. Geophys. Res.*, *108*(C5), 3144, doi:10.1029/
1072 1999JC000047.
1073 Sabine, C. L., and N. Gruber (2005), Response to comment on "the oceanic
1074 sink for anthropogenic CO_2," *Science*, *308*, 1743, doi:10.1126/
1075 science.1109949.
1076 Sabine, C. L., R. M. Key, K. M. Johnson, F. J. Millero, J. L. Sarmiento,
1077 D. W. R. Wallace, and C. D. Winn (1999), Anthropogenic CO_2 inventory
1078 of the Indian Ocean, *Global Biogeochem. Cycles*, *13*(1), 179–198.
1079 Sabine, C. L., R. A. Feely, R. M. Key, J. L. Bullister, F. J. Millero, K. Lee,
1080 T.-H. Peng, B. Tillbrook, T. Ono, and C. S. Wong (2002), Distribution of
1081 anthropogenic CO_2 in the Pacific Ocean, *Global Biogeochem. Cycles*,
1082 *16*(4), 1083, doi:10.1029/2001GB001639.
1083 Sabine, C. L., et al. (2004), The oceanic sink for anthropogenic CO_2,
1084 *Science*, *305*, 367–371.
1085 Sarmiento, J. L., J. C. Orr, and U. Siegenthaler (1992), A perturbation
1086 simulation of CO_2 uptake in an ocean general circulation model, *J. Geo-
1087 phys. Res.*, *97*(C3), 3621–3645.
1088 Schlitzer, R. (2004), Export production in the equatorial and North Pacific
1089 derived from dissolved oxygen, nutrient, and carbon data, *J. Oceanogr.*,
1090 *60*, 53–62.

1091 Takahashi, T. (2004), The fate of industrial carbon dioxide, *Science*, *305*,
1092   352–353.
1093 Takahashi, T., et al. (2002), Global sea-air CO_2 flux based on climatological
1094   surface ocean pCO_2, and seasonal biological and temperature effects,
1095   *Deep Sea Res., Part II*, *49*, 1601–1622.
1096 Tans, P. P., I. Y. Fung, and T. Takahashi (1990), Observational con-
1097   straints on the global atmospheric CO_2 budget, *Science*, *247*, 1431–
1098   1438.
1099 Taylor, K. E. (2001), Summarizing multiple aspects of model performance
1100   in a single diagram, *J. Geophys. Res.*, *106*(D7), 7183–7192.
1101 Wallace, D. R. (2001), Storage and transport of excess CO_2 in the oceans:
1102   The JGOFS/WOCE Global CO_2 Survey, in *Ocean Circulation and Cli-
1103   mate*, pp. 489–521, Elsevier, New York.
1104 Watson, A. J., and J. C. Orr (2003), Carbon dioxide fluxes in the
1105   global ocean, in *Ocean Biogeochemistry*, pp. 123–143, Springer,
1106   New York.
1107 Wilkin, J. L., J. V. Mansbridge, and J. S. Godfrey (1995), Pacific Ocean
1108   heat transport at 24°N in a high-resolution global model, *J. Phys. Ocea-
1109   nogr.*, *25*, 2204–2214.

———————————

1111   S. C. Doney, Marine Chemistry and Geochemistry, MS 25, Woods Hole
1112 Oceanographic Institution, 360 Woods Hole Road, Woods Hole, MA
1113 02543-1543, USA. (sdoney@whoi.edu)

   S. Dutkiewicz and M. Follows, Department of Earth, Atmosphere, and 1114
Planetary Sciences, Massachusetts Institute of Technology, 54-1412, 77 1115
Massachusetts Avenue, Cambridge, MA 02139, USA. (stephd@ocean. 1116
mit.edu; mick@ocean.mit.edu)   1117

   M. Gerber, F. Joos, and S. A. Müller, Climate and Environmental 1118
Physics, Physics Institute, University of Bern, Sidlerstr. 5, CH-3012 1119
Bern, Switzerland. (mgerber@climate.unibe.ch; joos@climate.unibe.ch; 1120
smueller@climate.unibe.ch)   1121

   N. Gruber, Department of Atmospheric and Oceanic Sciences, and 1122
Institute of Geophysics and Planetary Physics, University of California, 1123
5839 Slichter Hall, Los Angeles, CA 90024, USA. (ngruber@igpp. 1124
ucla.edu)   1125

   A. R. Jacobson, S. E. Mikaloff Fletcher, and J. L. Sarmiento, 1126
Atmospheric and Oceanic Sciences Program, Princeton University, Sayre 1127
Hall, Forrestal Campus, PO Box CN710, Princeton, NJ 08544-0710, USA. 1128
(andyj@splash.princeton.edu; sara@splash.princeton.edu; jls@princeton. 1129
edu)   1130

   K. Lindsay, Climate and Global Dynamics, National Center for 1131
Atmospheric Research, P.O. Box 3000, Boulder, CO 80307, USA. 1132
(klindsay@ucar.edu)   1133

   D. Menemenlis, ECCO, Jet Propulsion Lab, MS 300-323, 4800 Oak 1134
Grove Drive, Pasadena, CA 91109, USA. (menemenlis@jpl.nasa.gov) 1135

   A. Mouchet, Astrophysics and Geophysics Institute, University of Liege, 1136
Allée du 6 Août, 17 Bt. B5c, B-4000 Liege, Belgium. (a.mouchet@ 1137
ulg.ac.be)   1138